Polyaniline/gallic acid/cupric oxide nanocomposite with silver nanoparticles for increased photocatalytic degradation of 4-nitrophenol: structural, thermal and magnetic properties

P. Saravanan[a], N. Kalaivasan[b,*], E. Parthiban[c], J. Jayaprabakar[d]
[a]*Department of Chemistry, Anna University, Chennai, India.*
[b]*Department of Chemistry, Thanthai Periyar Government Institute of Technology, Vellore, Tamil Nadu, India*
[c]*Department of Chemistry, C. Abdul Hakeem College of Engineering and Technology, Melvisharam, Tamil Nadu, India.*
[d]*Department of Mechanical Engineering, Sathyabama Institute of Science and Technology, Chennai, India*

AgNPs@PANI/GA/CuO nanocomposites are formed up of embedded silver nanoparticles in polyaniline (PANI), gallic acid (GA), and copper(II) oxide. Using anhydrous iron trichloride (FeCl3) as an oxidant, gallic acid has been polymerized in situ in the presence of aniline monomers. To reduce silver nitrate ($AgNO_3$) and enable the integration of AgNPs onto the surface of the nanocomposite, Tridax procumbens leaf extract was utilised. A particulate size range of 50–10 nm for magnetic CuO nanoparticles was effectively added to the PANI-GA matrix. The AgNPs-decorated nanocomposite has been characterised via FT-IR, XRD, SEM, EDAX, TEM, and SAED, among other techniques. Vibrating sample magnetometry (VSM) and TGA/DTA analysis have also been used to investigate the magnetic, thermal, and biological properties of nanocomposites. Using sodium borohydride as a reducing agent, the catalytic qualities of the AgNPs@PANI/GA/CuO are studied about the reduction of 4-nitrophenol to 4-aminophenol.

(Received December 29, 2023; Accepted March 29, 2024)

Keywords: Photocatalytic activity, Catalysis, Gallic acid, Polyaniline plant extracts

1. Introduction

The removal of highly hazardous nitro aromatic compounds and dyes from industrial wastewater is a topic of great interest nowadays. Removing these compounds rigorously using conventional reduction systems leads to an increase in their chemical and biological stability. Because hazardous nitro aromatic chemicals are employed in so many different industries, including textiles, paints, plastics, explosives, drugs, and industrial solvents, there is no substitute for them in human existence. 4-nitrophenol 4-NP (4-nitro phenol) is a mono nitro phenol which is carcinogenic to living things. It accumulates in foods and affect human and animal blood components' liver, skin, kidney, respiratory tracts, and central nervous systems, leading to several deadly disorders, including methemoglobinemia [1]. Human intake of 4-NP could result in symptoms like cyanosis, vomiting, unconsciousness, and stomach pain. Environmental stability, non-biodegradability, ease of saturation to subsurface water through soil, and excessive concentration to surpass the highest probability of only 10 ppb in natural water are the main features of 4-NP. Since 4-NP may be efficiently eliminated through degradation, 4-AP (4-aminophenol) is a reduction component being safer than the original molecule, it finds use in the production of dyes, photographic developers, corrosion inhibitors, and medicines with antipyretic and analgesic effects [2–3].

* Corresponding author: nkkvasan78@gmail.com
https://doi.org/10.15251/DJNB.2024.191.459

Because of their remarkable physical, chemical, and biological characteristics, noble metal nanoparticles are currently being actively used in a variety of human activity-related research domains, including biomedicine, biological imaging, optoelectronics, agriculture, photocatalysis, and energy conversion [4]. Additionally, the high unambiguous surface area and catalytic execution of the nanoparticles, tend to steadily increase with decrease in nanoparticle size, made them useful for the catalysis of several types of reactions. Silver nanoparticles, also known as AgNPs, are particularly important due to their relative abundance, low price, highly conductive (both thermal and electrical), Antimicrobial properties and high oxidation resistance. As a result, they are finding use in burn dressings, food additives, textiles, and healthcare products [5–6]. Polyaniline has been the most significant conducting polymer because of its tuneable conductivity, mechanical stability, nontoxicity, low cost, simply synthesized, reversible doping/dedoping process, environmental stability, π-electron conjugated structure, controllable electrochemical, and chemical properties. Currently, polyaniline nanostructures with nanorods, nanowires, nanotubes, and nanoparticles have been more fascinated with an advance in nanotechnology [7]. In addition, PANI can be used in the preparation of batteries, catalysis, sensors, electronic devices, light-emitting diodes, anti-corrosion coatings, and in biomedical applications like biosensors, targeted drug delivery, cardiac, neural probes, tissue engineering, and antimicrobial activity [8-10].

Gallic acid (GA, 3,4,5-trihydroxy benzoic acid) is a white solid powder, which can be found in sumac, gallnuts, tea leaves, oak bark, grapes, bananas, strawberries, and other plants. GA contains three hydroxyl groups and a carboxylic acid group added to a benzene ring. It is a naturally occurring polyphenolic metabolite that is non-toxic, biodegradable and has a variety of industrial uses such as cosmetics, the antioxidant in food, pharmaceutical, tanning, ink dyes, manufacture of paper, oxygen scavenging, radioprotective activity, and therapeutic agent, etc., [11-13]. In recent years, green chemistry approaches for the fabrication of metallic (like Au, Ag, Pb, Pt, Cu, Fe) and metal oxides such as Fe_3O_4, TiO_2, SnO_2, CuO, ZnO from natural ingredients, to avoid the problems related to toxic chemicals and solvents. The use of biological materials such as plant extracts leaves, stem bark, flowers, seed, roots, and fruit peels have promoted the synthesis of metal nanoparticles without solvents [14]. The Tridax procumbens (Coat buttons) leaf act as an excellent reducing agent that includes antioxidant, flavonoid, and other chemical compounds such as alkyl esters, sterols, fatty acids, pentacyclic triterpenes, and polysaccharides. It has been commonly used in traditional (Ayurvedic) medicine in India for wound healing, liver disorders, boils, gastritis, hepatoprotection, blisters, heartburn, antifungal, anticoagulant, and insect repellent [15-16]. Cupric oxide or Copper(II) oxide (CuO) is an inorganic compound with a black solid containing two stable oxides of copper. Tajik et al. have studied the Fe_3O_4/CuO nanoparticles through a sensitive electrochemical technique. Photocatalytic degradation of ZnO/CuO composite, Gr-CuS-ZnO, and CS-PANI-CuO hybrid nanocomposite has also been discussed [17-20]. Antibacterial and anticancer activity of Ag/TiO_2 and Ag/SiO_2 composite and polyaniline-TiO_2-polyaniline core-shell nanocomposite has been studied. The green synthesis of Ag nanoparticle decorated tea polyphenols/graphene (Ag-TPG), AgNPs-GO-TiO_2, and LaNiSbWO4-G-PANI nanocomposite for catalytic reduction of Congo red dye and 4-nitrophenol[1-2, 21-22].

The present work aimed to develop a new kind of polymeric silver nanoparticles decorated with magnetic and thermal sensitive polyaniline-gallic acid-copper oxide nanocomposite. Following that, gallic acid and polyaniline skeletons' hydroxyl and amino groups were important in chelating silver ions to enhance their reduction and produce AgNPs on the composite's surface. The silver nanoparticles prepared from Tridax procumbens leaf extract an eco-friendly greener approach by biotic resources plant extract have been examined. The prepared nanocomposite was characterized via various analysis techniques including FT-IR, XRD, TGA/DTA, UV-visible spectra, SEM, TEM, EDAX and VSM to investigate their thermal stability, structural, and magnetic properties. Further, the photocatalytic reduction reaction of toxic 4-nitrophenol to 4-aminophenol was examined to clarify the photocatalytic activity of the AgNPs@PANI-GA-CuO nanocatalyst.

2. Experimental

2.1. Chemicals

Aniline, gallic acid, and silver nitrate ($AgNO_3$) were procured from Sigma Aldrich, India. Merck, India supplied the hydrochloric acid (HCl), sodium hydroxide (NaOH), ethanol, and ammonia in a 25% solution. 4-nitrophenol (4-NP), and copper(II) oxide (CuO) was procured from Sisco Research Laboratories, India. The fresh leaves of *Tridax procumbens* (Family: Asteraceae) were gathered from Melvelam village, Ranipet, Tamil Nadu, India.

2.2. Fabrication of PANI/GA/CuO nanocomposite

To get a homogenised solution, 0.2 mol of gallic acid was dissolved for 30 minutes of vigorous stirring in double distilled water. After that, 0.2 mol of aniline was added, and the mixture was continuously stirred mechanically for an hour. The mixture including aniline monomer and acid was added dropwise to 0.2 mol of anhydrous $FeCl_3$ solution in an ice bath for 30 minutes. The polymerization reaction was then carried out by stirring the mixture overnight at 5–10°C. The polyaniline-doped gallic acid with CuO nanocomposite was then dried at 60°C in an oven for a day after being filtered through a funnel.

2.3. Preparation of silver nanoparticles (AgNPs)

To get rid of any apparent dust and undesired particles, the leaves of *Tridax procumbens* (TP) were gathered and carefully washed in double distilled water. 15 grams of finely chopped *Tridax procumbens* (TP) leaves were placed in a conical flask, and after 12 minutes of boiling in 150 mL of double-distilled water, the plant extract was collected and kept at 4°C using Whatman filter paper no. 40. Ten ml of *Tridax procumbens* leaf extract was added to a 20 ml aqueous solution of silver nitrate (1 mg) while it was being stirred mechanically for two hours. Silver nanoparticles were seen as a typical yellowish-brown colour change in the solution. The colour changed from colourless to colloidal brown, indicating that $AgNO_3$ was completely reduced to Ag^0. The relative composition details of the prepared nano composites are presented in *Table 1.*

Table 1. Relative composition of the reaction mixtures for the fabrication of AgNPs@PANI/GA/CuO nano composite based on ANI, GA, $FeCl_3$, CuO, TPLE and $AgNO_3$.

S. No	Sample code	Feed composition					
		ANI (mol)	GA (mol)	$FeCl_3$ (mol)	CuO (mol)	TPLE (mL)	$AgNO_3$ (mL)
1	$SA_1G_3C_4$	0.1	0.3	0.4	0.05	10	20
2	$SA_2G_2C_4$	0.2	0.2	0.4	0.05	10	20
3	$SA_3G_1C_4$	0.3	0.1	0.4	0.05	10	20
	TPLE- Tridax Procumbens Leaf Extract, GA-Gallic acid, ANI-Aniline						

2.4. Fabrication of AgNPs@PANI/GA/CuO nanocomposite

After washing with distilled water, the PANI/GA/CuO nano composite is added with 50 mL of 0.5M ammonium hydroxide for total deprotonation. Two grams of the previously deprotonated nanocomposite were added to 60 ml of AgNPs solution and agitated mechanically for 31/2 hr. The resultant nanocomposite washed out six times using ethanol and double-distilled water before being dried for 48 hours at 60°C in an oven for further analysis. The mechanism displays, the in-situ polymerisation of polyaniline into gallic acid solution followed by the in-situ formation of CuO in the gallic acid-polyaniline matrix in Fig. 1.

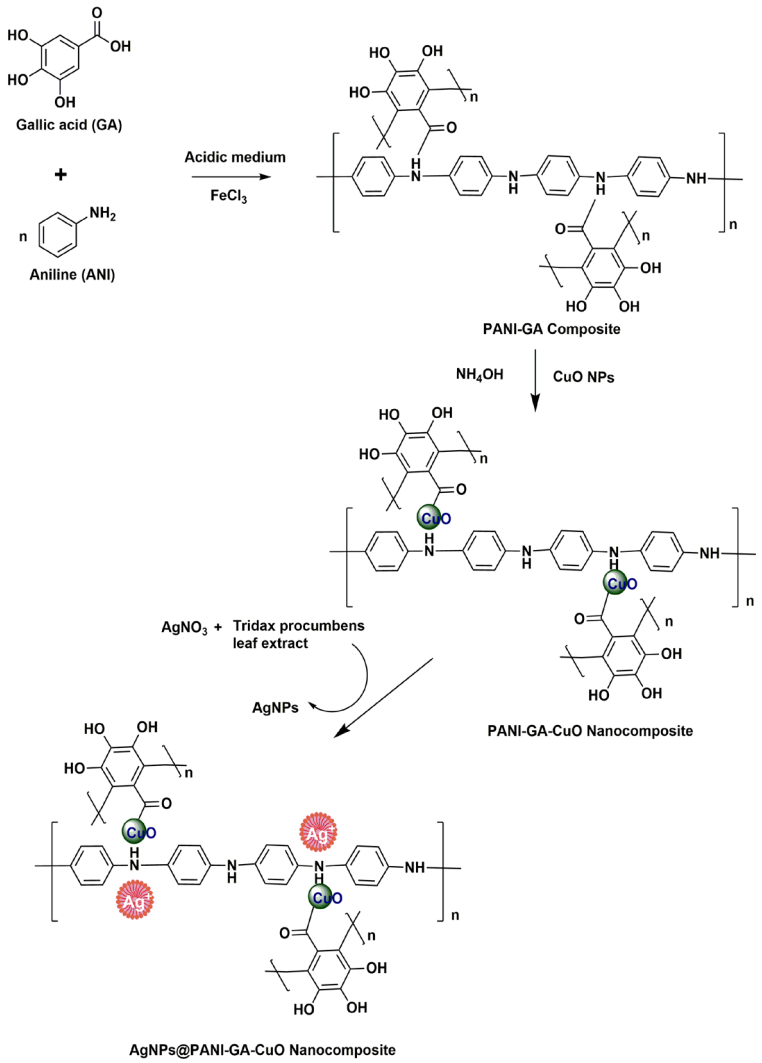

Fig. 1. Formation of AgNPs@PANI/GA/CuO nanocomposite via in-situ polymerization.

2.5. Catalytic activity of prepared nano composite

A standard catalytic reaction for the degradation of 4-nitrophenol was conducted in a quartz cuvette that had been well-stoppered. The UV-VIS absorption spectra is acquired after adding 2.5 mL (7 mM) of an alkaline solution of 4-nitrophenol, 0.5 mL (10 mg/l) of sodium borohydride (NaBH4), and 1 mg of AgNPs@PANI/GA/CuO nanocomposite to the initial solution.

2.6. Characterisation

The crystallinity and phase composition of the nano composite are studied using X-ray diffraction patterns recorded on an TTK 450 powder (Anton Paar with Cu-Kα radiation (Bruker AXS D8 Advance). FT-IR spectra were recorded functional groups of nanocomposites using Alpha Bruker-2009 spectrophotometer by the KBr pellet frequency range at 400-4000 cm^{-1} at 2 cm^{-1} resolution. Thermo gravimetric analysis (TGA) was made (SEIKO model TG/DTA 6200 in nitrogen environment) and magnetic study conducted with vibrating sample magnetometer (VSM, Lake Shore 7404). Transmission electron microscopy (using the LaB6 JEM 2000 model) and the JSM-6701S SEM microscope were used to examine the surface architecture of the nanocomposite. Using an EDX spectrometer (Philips model XL30), the elemental composition of the samples of nanocomposite material was assessed. UV–VIS absorption spectrum was recorded using a Double beam Shimadzu UV-2550 spectrophotometer range (200–800 nm).

3. Results and discussion

3.1. FT-IR spectral studies

Fig. 2 shows the FT-IR spectrum of polyaniline, gallic acid, PANI/GA/CuO, and AgNPs@PANI/GA/CuO nanocomposite, where the wave number (cm^{-1}) is plotted as a function of percentage transmittance. From Fig. 2a, it can be seen that absorption peaks of polyaniline were observed at 1571 cm^{-1} (quinoid ring), 1460 cm^{-1} (benzenoid ring), 1262 cm^{-1} (C–N vibration of quinoid-benzenoid-quinoid), 1086 cm^{-1} (C–H in-plane), and 811 cm^{-1} (C–H out-of-plane), respectively [23]. Gallic acid characteristic peaks at 3278 cm^{-1} are assigned to the O–H stretching. The vibrational spectra for gallic acid confirm an effective protonation of the characteristic band of carbonyl stretching (C=O) at 1703 $cm^{-1.}$ As seen in Fig. 2b, further typical modes include the out-of-plane bending of the hydroxyl group at approximately 1428 cm^{-1}, the stretching of the phenolic groups (C-OH) at 1010 cm^{-1}, and the aromatic ring stretch (C=C) at 1604 cm^{-1} [24]. Owing to the copper oxide nanocomposite, two prominent peaks can be seen at 491 and 667 cm^{-1}. The interaction between polyaniline and gallic acid is indicated by the rise in the PANI/GA/CuO nanocomposite's spectrum between 3475 cm^{-1} and 2300 cm^{-1}. Furthermore, the effective interaction between polyaniline and gallic acid is demonstrated by the disappearance of gallic acid peaks at 1428 cm^{-1} and the emergence of a new peak for the PANI-GA-CuO nanocomposite (Fig. 2c) at 1638 cm^{-1} [25–26].

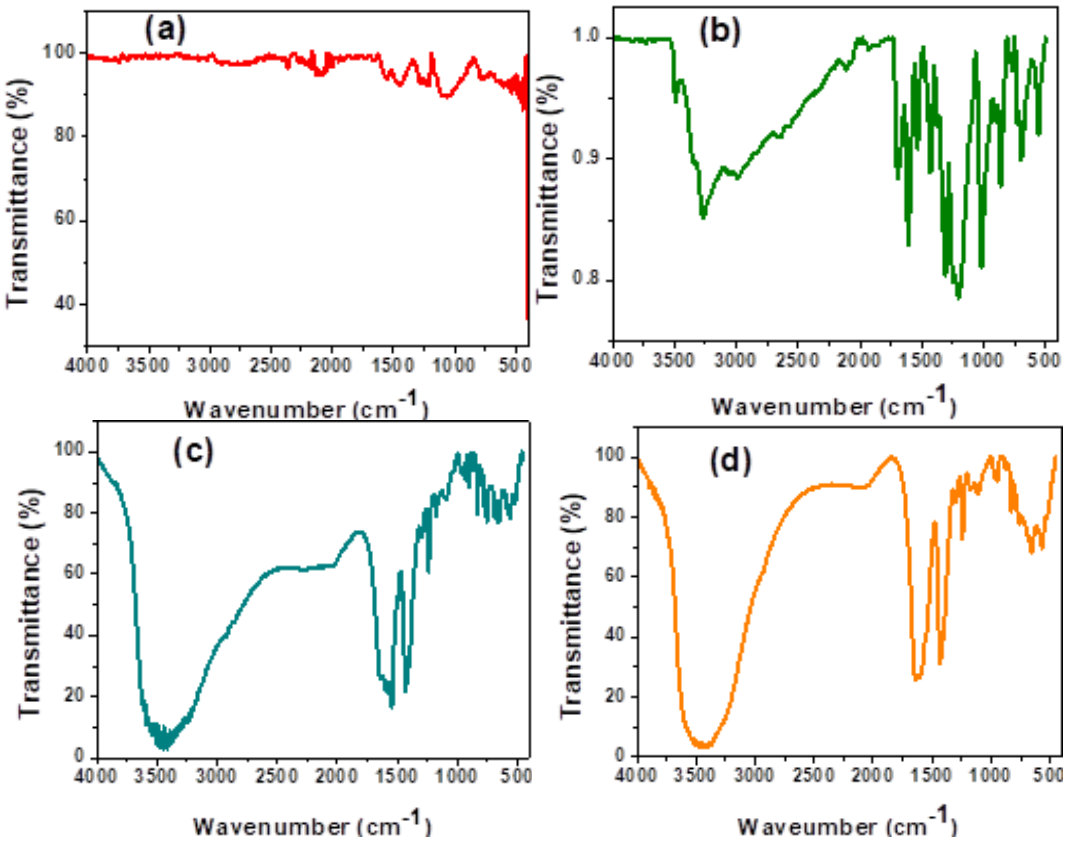

Fig. 2. FT-IR spectrum of (a) PANI, (b) GA, (c) PANI/GA/CuO, and (d) AgNPs@PANI/GA/CuO nanocomposites.

A new peak at 558 and 1090 cm^{-1} was supported by the creation of a vibrational copper oxide (Cu-O) bond. The dopant anion vibration band and the C–N^{+} stretching in the Ar–N peak at 1243 and 1174 cm^{-1} are responsible for the polyaniline–gallic acid observed peak at 1066 cm^{-1}. The stretching vibration of the Cu-O bond and the interaction between polyaniline-doped gallic

acid and copper oxide result in the presence of fresh peaks at 1583 cm^{-1}. The polymer Cu NCs have also caused peaks to shift and move to 1418, 1230, 1090 and 745 cm^{-1} respectively. Because of the Ag metal reduction of the nanocomposite, the presence of amino groups (-NH) and hydroxyl groups (-OH) causes a shift in position at 1430 and 3475 cm^{-1} to 1418 and 3454 cm^{-1}. (Fig. 2c and Fig. 2d) [27-28]. Excellent interaction between polyaniline, gallica acid, copper oxide, and AgNP inclusion on the PANI/GA/CuO nanocomposite is demonstrated by the FT-IR.

3.2. Thermal (TGA-DTA) properties

The TG thermograph of polyaniline doped with gallic acid nanocomposite could be speciously divided into multi-steps of weight loss (Fig. 3). Due to the elimination of water molecules from the polymer matrix, the first stage samples PANI/GA/CuO and AgNPs@PANI/GA/CuO lost weight at temperatures between 100 and 151°C and 81 and 152 °C, respectively, while the second weight loss in temperature range from 200 to 512°C and 181 to 460 °C due to cleavage of polymeric chain network of gallic acid. The final decomposition was observed at 700 to 786 °C and 458 to 789 °C due to the breaking of the polyaniline chain (Fig. 3a) and (Fig. 3b). The thermal analysis exposed copper oxide (CuO) nanoparticles could be retarding the decomposition of polyaniline chain to the higher temperature. The entire weight loss of the PANI/GA/CuO and AgNPs@PANI/GA/CuO nanocomposite is 56.92 and 43.08%, respectively, with the residue of copper oxide (CuO) being 42.88 and 57.12 % [29–31]. Generally, it can be concluded that the PANI/GA/CuO and AgNPs@PANI/GA/CuO nanocomposite's thermal stability is enhanced by gallic acid's accessibility.

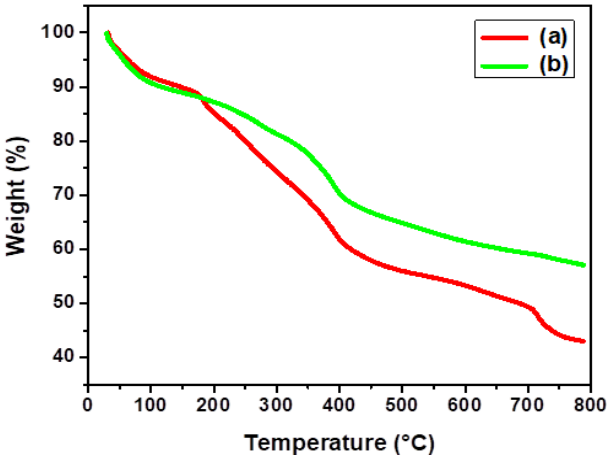

Fig. 3. Thermogravimetric (TGA) curves of (a) PANI/GA/CuO, and (b) AgNPs@PANI/GA/CuO nanocomposites.

Fig. 4a shows the thermal (DTA) curves of the PANI/GA/CuO nanocomposite. The expulsion of water molecules for the crosslinking of the polyaniline polymeric chain resulted in the observation of the endothermic peak at 191.79 °C within the temperature range of 173.81 to 219°C [32]. AgNPs@PANI/GA/CuO nanocomposite, as depicted in Fig. 4b, exhibits a comparable endothermic peak at 62 to 130°C and sharp peaks appeared at 77.83°C because of the polymer chain network, strong binding of the silver nanoparticles, and trace amounts of water moieties [33–34]. From the above analysis it has been concluded that the PANI/GA/CuO begin weight loss at lower temperatures than the AgNPs@PANI/GA/CuO nanocomposites.

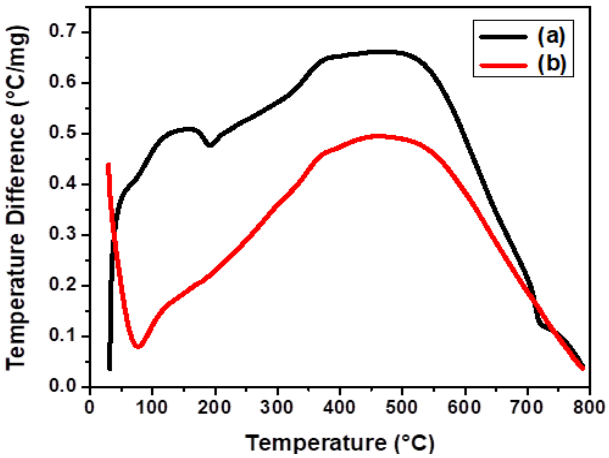

Fig. 4. Differential thermogravimetric (DTA) curves of (a) PANI/GA/CuO, and (b) AgNPs@PANI/GA/CuO nanocomposites.

3.3. X-ray diffraction studies

Fig. 5a, 5b, and 5c show the X-ray diffraction patterns of polyaniline, PANI/GA/CuO and AgNPs@PANI/GA/CuO nanocomposite. From Fig. 5a, it can be seen that the XRD patterns of polyaniline show a diffraction peak with 2θ at 15° (011), 20° (100), 25° (110), and 35° (200) are observed to the periodicity parallel and perpendicular to the polymer chain of polyaniline (Standard JCPDS No: 053-1890). Because CuO nanoparticles are mostly crystalline, the resulting nanocomposite PANI/GA/CuO exhibits patterns of CuO that may be indexed to two strong peaks at 2θ = 35.80° and 39.84°. The (h k l) reflection peaks of [110], [002], [111], [202], [020], [202], [113], [311], [113], and [311] at 2θ equivalent to 32.83°, 35.80°, 39.84°, 48.93°, 53.59°, 61.64°, 66.25°, 68.48°, and 75.50° (JCPDS No:48-1548) respectively (Fig. 5b). After formation of AgNPs over its surface represents PANI/GA/CuO nanocomposite [35-36]. Four diffraction lines, corresponding to 38.80°, 46.40°, 66.24°, and 75.44°, can be observed in Fig. 5c. These lines may be indexed to the lattice plane of face-centered cubic Ag crystals [111], [200], [220], and [311] [6, 37]. An attained XRD diffractions coincide with Infrared (FT-IR) spectrum results and therefore confirm the formation of copper oxide and AgNPs of PANI/GA/CuO nanocomposite.

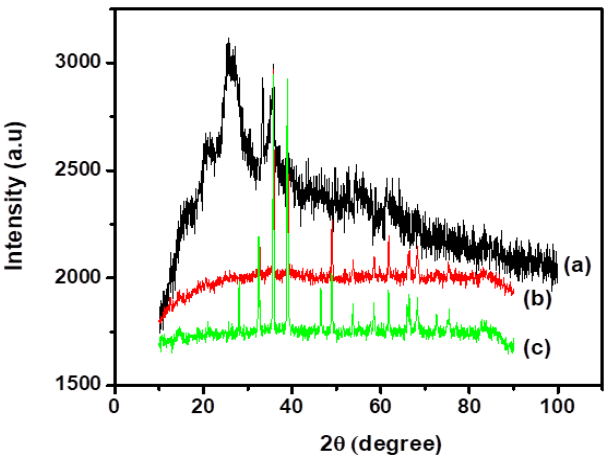

Fig. 5. X-ray diffraction pattern for nanocomposites.

3.4. Magnetic (VSM) properties

Fig. 6 shows the magnetic curves of copper oxide (CuO) with an applied magnetic field at room temperature. Since, the conducting polymer polypyrrole, polyaniline, and polythiophene are not magnetic, the magnetic characteristics of prepared AgNPs@PANI/GA/CuO nanocomposites are strongly dependent on the content of copper oxide NPs. The magnetic hysteresis loops, the saturation magnetization value was obtained at 0.0030 emu/g for the above paramagnetic behaviour of AgNPs@PANI/GA/CuO nanocomposite [23, 25, 38]. The interaction between the polyaniline polymer chain and CuO has been seen in magnetic AgNPs@PANI/GA/CuO nanocomposites. This interaction is enhanced by the hydrogen bonding between CuO's –O– and –N– of PANI.

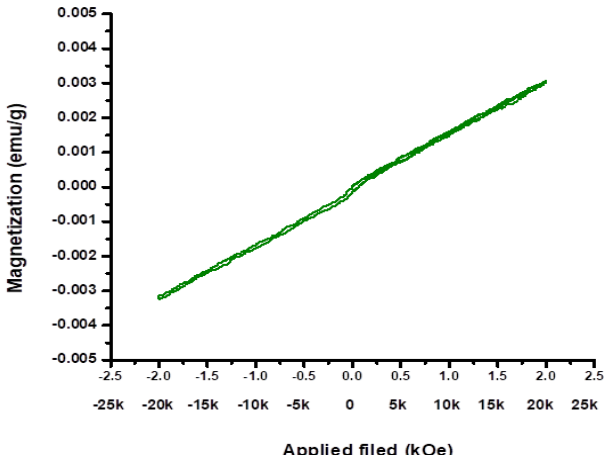

Fig. 6. Magnetization curves of AgNPs@PANI/GA/CuO nanocomposite.

3.5. SEM and EDAX analysis

The particle size and surface morphology of the proposed nanocomposite, which contains different concentrations of copper oxide nanoparticles, are determined by scanning electron microscopy. From Fig. 7a, it is revealed that the surface morphology of nano composite, which shows the CuO–Ag nanostructures' granular structure of rough, porous, and with voids without aggregating on the polyaniline-gallic acid matrix, with an average diameter of 50 µm. It has been informed that the in-situ polymerization of aniline with anhydrous Iron(III) chloride in an acidic medium produces coarse particles with rough shapes [34-35].

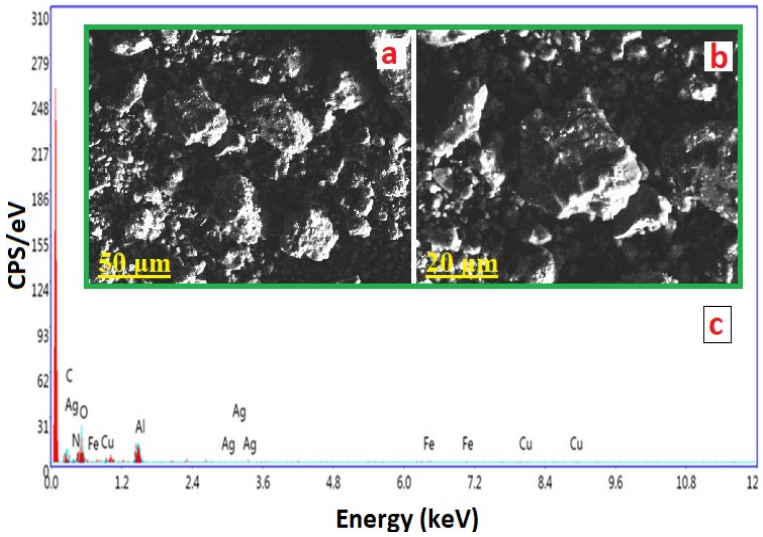

Fig. 7. a) SEM micrographs and b) EDAX image of AgNPs@PANI/GA/CuO nanocomposite.

The EDAX spectra of silver nanoparticles incorporated PANI/GA/CuO nanocomposite exhibited the formation of chemical composition and weight percentage of oxygen, carbon, nitrogen, and metal ions like copper, iron, and silver (Fig. 7b). The weight percentage of oxygen-51.09%, carbon-22.68%, nitrogen-7.37%, copper-4.92%, iron-2.53% and silver-1.37% and atomic percentage oxygen-50.85%, carbon-32.41%, nitrogen-8.38%, copper-1.48%, iron-0.72% and silver-1.05% were calculated from EDAX. The results obtained demonstrated that AgNPs and CuO were present across a polyaniline-gallic acid polymer matrix.

3.6. TEM morphology

Fig. 8 shows the TEM micrograph images that were used to investigate the particle size and silver nanoparticles and they are distributed uniformly within AgNPs@PANI/GA/CuO nanocomposite using LaB6 JEM 2000 model. Transmission electron microscopy image of PANI-GA-CuO NCs (Fig. 8a-b) shows the dispersion of copper oxide and silver nanoparticles through a polyaniline-gallic acid matrix with low aggregation at magnification. After the incorporation of AgNPs, the images of PANI-GA-CuO nanocomposite show moon, circle, and spherical-shaped structure due to the formation of CuO nanoparticles and AgNPs with a particle size range between 50 and 10 nm. From Fig. 8c, it can be seen that the high-resolution TEM image confirmed the formation of CuO nanoparticles in AgNPs@PANI/GA/CuO nanocomposite [33, 38]. The interplanar spacing of approximately 0.210 nm in between the strips indexed to lattice plane [111], [200], [220], and [311] of silver nanoparticles is characterised by lattice fringes coherently stretched over each nanocomposite. The bright circle rings that make up the Selected Area Electron Diffraction (SAED) pattern have been used to provide structural and crystallinity information about CuO nanoparticles that is dependable on the results found from the XRD pattern (Fig. 8d).

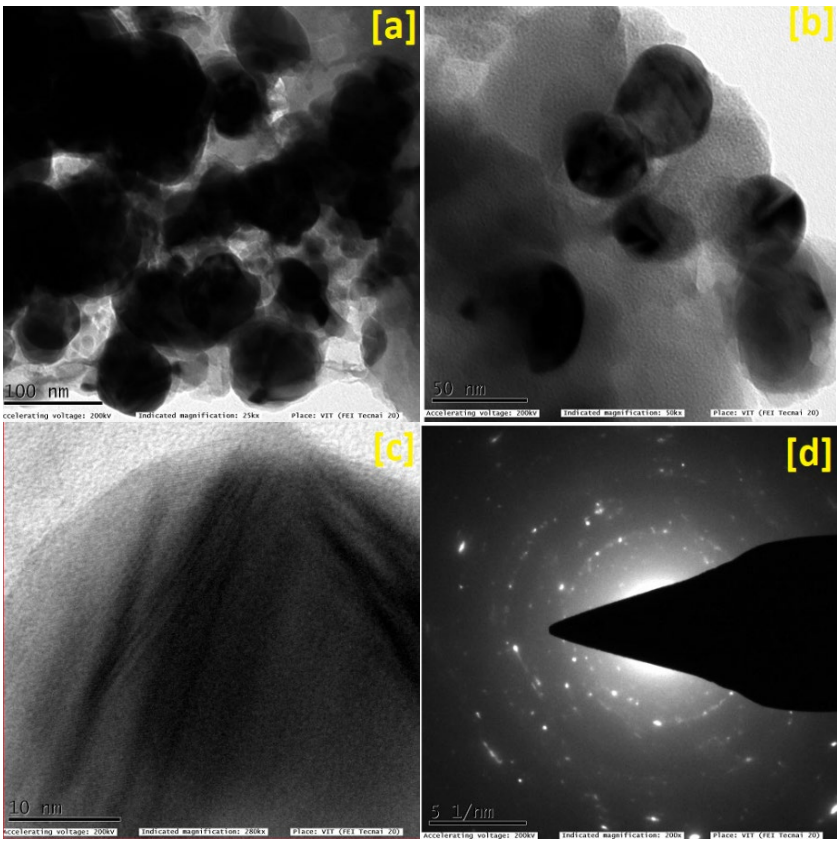

Fig. 8. a) TEM images b) HRTEM c) SAED of AgNPs@PANI/GA/CuO nanocomposite.

3.7. Catalytic study

Silver nanoparticles (AgNPs) were supported into various substrates such as gallic acid (GA) and polyaniline (PANI) were explored as a catalyst for many reactions. In their biogenic report on the nanocomposite study, Nasrollahzadeh et al. developed a nanocomposite of Ag, RGO and TiO_2 from plant extract and tested it against three organic dyes at room temperature. This makes it possible to create novel, environmentally friendly nanocomposites that may be used in a variety of industries [1]. One of the catalytic features of the AgNPs@PANI/GA/CuO nanocomposite that was selected for example was the reduction of 4-nitrophenol (4-NP) to 4-aminophenol (4-AP). Reducing agents of sodium borohydride ($NaBH_4$) can be reduced from 4-NP to 4-AP. The objective of noble metal nanoparticles' catalytic activity is to hasten electron transmission from donor borohydride (BH4−) to the acceptor 4-nitrophenol (4-NP). The reaction is expected to proceed, resulting in the development of two reactive types, Ag-BH3− and Ag-H, as shown in equation (1). When sodium borohydride was added to a 4-nitrophenol solution, Fig 9 equations (2)–(6) demonstrated a Langmuir–Hinshelwood mechanism that verified the participation of AgNPs in the catalytic reaction. Even after many days, the absorption intensity did not change, suggesting that the addition of a catalyst is required to speed up the reaction and then monitor its development [2].

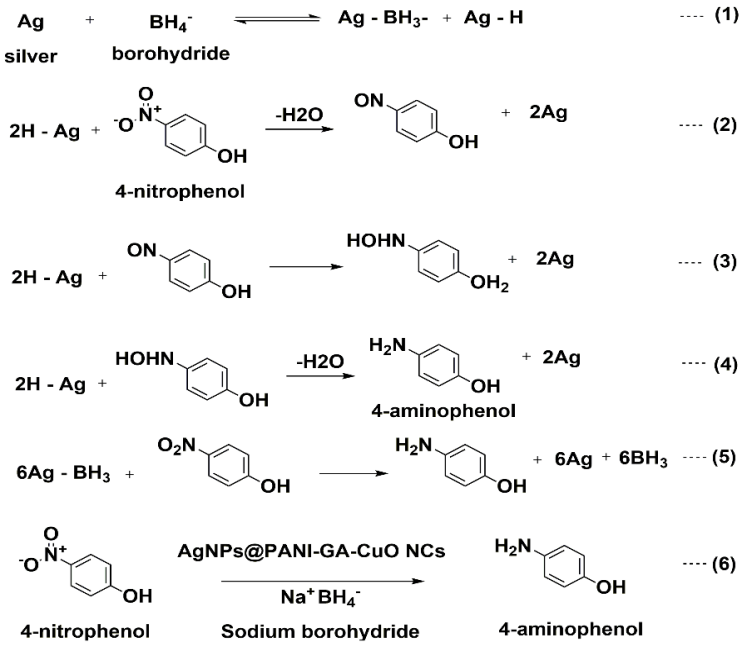

Fig. 9. The mechanism of the catalytic reduction of nitrophenol at room temperature.

The reaction proceeded satisfactorily after the addition of AgNPs@PANI/GA/CuO nanocomposite to 4-NP in the presence of NaBH4. The absorption peak of 4-NP at 400 nm reduced to 4-AP was observed by altering the intense yellow colour of 4-NP, which gradually vanished due to the formation of the 4-AP solution over time. Furthermore, a novel peak associated with the reduction product 4-AP appeared at 310 nm. Moreover, the decrease in absorbance at 400 nm with time, as illustrated in Fig. 8, can be used to determine the degradation in the concentration of 4-NP. The catalysis test was conducted using 1 mg and 2 mg of AgNPs@PANI/GA/CuO nanocomposite to investigate its effects. The results show that the reaction was completed in 16 and 8 minutes, respectively, as shown in Figs 10a and 10b [3]. Fig. 11a illustrates how the concentration of 4-NP decreases over time. The kinetic rate of the reduction reaction was determined using the pseudo-first-order kinetic model because the high concentration of the reducing agent, sodium borohydride, was significantly lower than that of 4-NP. Plotting the linear connection between ln At /Ao and time (t), where At is the absorbance at time t and Ao is

the starting absorbance, is done using a pseudo-first-order kinetic model, as shown in Fig 11b. The synthesized AgNPs@PANI/GA/CuO heterogenous nanocatalyst exhibited a high rate of reaction up to 0.20417 min−1 [42].

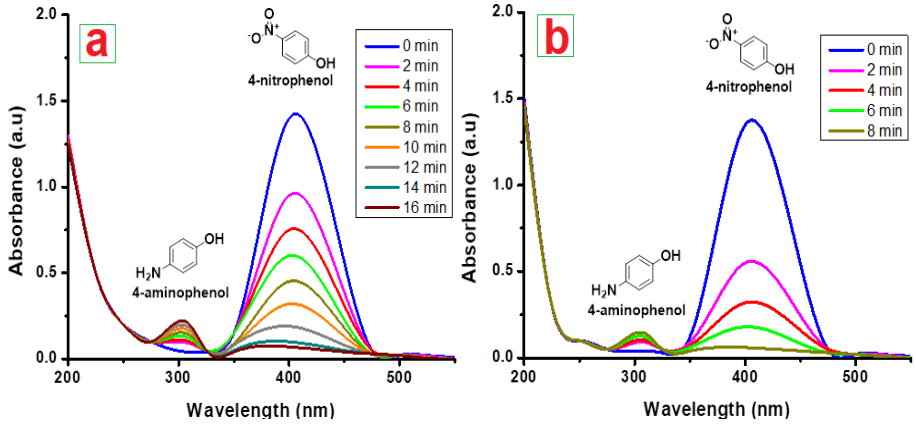

Fig. 10. UV-visible spectra recorded during the reduction of 4-NP to 4-AP by $NaBH_4$ a) 1 mg b) 2 mg of AgNPs@PANI/GA/CuO nanocatalyst.

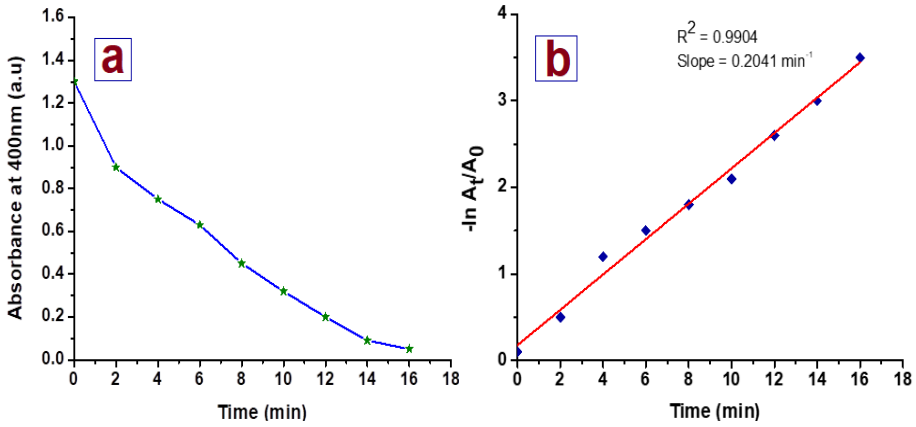

Fig. 11. a) Time dependent absorbance change for the reduction of 4-NP to 4-AP by $NaBH_4$ presence of AgNPs@PANI/GA/CuO nanocatalyst b) -ln A_t/A_0 versus the reduction reaction time.

Table 2 summarises the kinetic rates of several noble metals decorated onto various catalytic substrates, with the calculations based on pseudo-first-order model. These Ag NPs are anchored onto a variety of supporting substrates, such as poly [N-(3-trimethoxysilyl) propyl] aniline, RGO/TiO2, TPG nanohybrid, and PANI nanocomposite, in addition to p(AMPS). Elements include Pd, Cu, Fe, Ti, and Si. [1-2, 42]. A thorough comparison of our system's results with those of previous studies makes it clear that in contrast with huge quantities of other catalytic substrates at higher doses, a high catalytic reaction rate was achieved with a relatively little amount (1 mg) of AgNPs@PANI/GA/CuO nanocomposite. The tiny size of the AgNPs that are evenly dispersed within the PANI/GA/CuO nanocomposite low dosage catalyst may account for the remarkable catalytic activity. The presence of chelating sites in both polyaniline (PANI) and gallic acid (GA), denoted in amino groups (-NH2) and hydroxyl groups (-OH), is ensnaring more silver nanoparticles important to an increase in decorating silver metal onto a small weight of the catalyst. Compared to other catalyst systems, Table 2 shows how simple it is to separate the catalyst and how little (1 mg) catalyst is needed.

Table 2. Comparison the catalytic activity of silver nanoparticles decorated onto various catalytic substrates for the reduction of 4-NP to 4-AP with $NaBH_4$ reported in the literature.

Catalysts	Dose	Reduction rate (10^{-3} S^{-1})	Ref.
Ag/RGO/TiO_2 nanocomposite	0.05 mmol	3.15	[1]
AgNPs-TPG nanohybrid	10 mmol	3.35	[2]
AgNPs/poly[N-(3-trimethoxysilyl) propyl] aniline	7.2 mg	3.17	[42]
Fe_3O_4@SiO_2-Ag	1 g	7.67	[43]
Pd@PANI-CS-Fe_3O_4	1 mg	3.7	[44]
AgNPs@PANI/GA/CuO nanocomposite	1 mg	4.70	*Present study

One milligram of the developed nano-catalyst was used to assess the catalyst's recovery under the same circumstances as above. To preserve this little amount of nano-catalyst during separation, the nano-catalyst was subjected to a magnetic field in the reaction vessel. The generated 4-aminophenol was gradually collected with a syringe. To confirm that the catalyst is complete, it was recovered four times without losing any of its effectiveness. The recycling reduction process percentage in the first is 98%, but the recycling percentages in the second, third, and fourth are 97%, 95%, and 93%, respectively (Fig. 12). The four recycling techniques' time differences demonstrate a slight decline in catalyst efficiency, which may be related to just a little of substrate loss during the recycling process. Zhang et al. presented a mathematical approach (1) that was used to compute the efficiency of recovery times [45].

$$\propto = \frac{Co-Ct}{Co} \text{ X } 100 \quad (1)$$

where Co and Ct are the concentration at initial and final stages respectively. The efficiency percentages throughout the course of four consecutive cycles, with the fourth cycle having an efficacy of over 95%. This indicates that there will be very little loss in catalytic efficacy when the catalyst is being used in the same amount multiple times.

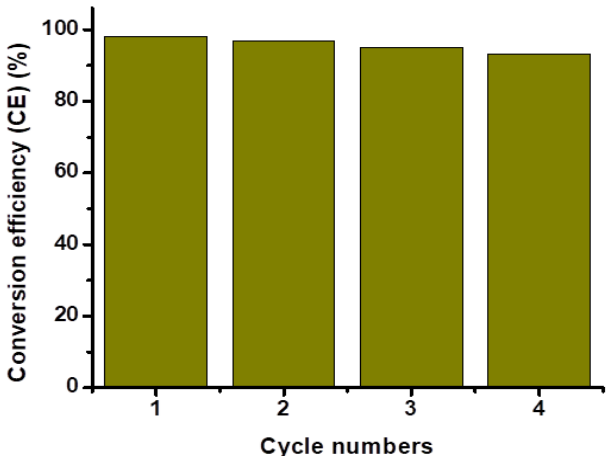

Fig. 12. Reusability of AgNPs@PANI/GA/CuO nanocomposite.

Moreover, the preparation of polyurethanes, plastics, pesticides, dyes, explosives (2,4,6-trinitrophenol and 2,4,6-trinitrotoluene), as well as some pharmacological medicine (4-R- 2-nitrophenol derivatives, R = H, CH3, OCH3, CF3), results in the production of the majority of these nitro aromatic chemical compounds. There is a growing need to use nanocomposite for applications involving amino aromatic compounds, which are less hazardous than nitroaromatic

compounds. Therefore, it is important to monitor AgNPs@PANI-GA-CuO nanocomposite's photocatalytic behaviour in the future about the reduction of some of the abovementioned compounds. The impact of various substituents (electron-withdrawing and electron-repelling groups) at different locations in the nitro aromatic and nitro aliphatic moieties on the catalytic reduction behaviour of the nanocomposite will be investigated.

4. Conclusion

To summarize, we have effectively created a straightforward and environmentally friendly approach for creating PANI/GA/CuO nanocomposite by in-situ polymerization utilizing aniline, with iron (III) chloride functioning as an oxidizing agent when gallic acid is present. The polyaniline-gallic acid NCs substrate is essential for the reducing control of polyaniline and the accessibility of hydroxyl, amino, and imino groups in GA and PANI. This allows for the easier synchronization of these basic active regions of silver ions. AgNPs@PANI/GA/CuO was characterized by XRD, FT-IR, SEM/EDAX, TEM, TGA/DTA, VSM, HRTEM, and SAED both before and after the AgNPs were decorated. The successful existence of AgNPs@PANI/GA/CuO NCs with a moon, circle, and spherical-shaped structure and a particle size range of 50–10 nm was validated by these characterizations. The synthesized AgNPS@PANI/GA/CuO nanocomposite shown a high degree of catalytic effectiveness in reducing 4-nitrophenol (4-NP) to 4-aminophenol (4-AP), as demonstrated by the UV-visible spectra. Additionally, using magnetic separation, the newly created nanocomposite made of conducting polymer polyaniline and natural compound gallic acid with AgNPs has been deemed an environmentally friendly nanocomposite. AgNPs@PANI-GA-CuO nanocomposite has the potential to be a useful catalyst for the reduction of 4-NP used in industry.

Acknowledgements

The authors thank the Department of chemistry, Anna University for providing the laboratory facilities and Dr. E. Parthiban, of C. Abdul Hakeem College of Engg and Tech, Ranipet for the necessary Instrumentation facilities.

References

[1] M. Nasrollahzadeh, M. Atarod, B. Jaleh, M. Gandomirouzbahani, Ceramics International 42(7), 8587 (2016); https://doi.org/10.1016/j.ceramint.2016.02.088

[2] Z. Wang, C. Xu, X. Li, Z. Liu, Colloids and Surfaces A: Physicochemical and Engineering Aspects 485, 102 (2015); https://doi.org/10.1016/j.colsurfa.2015.09.015

[3] F. Liu, X. Liu, W. Liu, H. Gu, Polymer 219, 123539 (2021); https://doi.org/10.1016/j.polymer.2021.123539

[4] K. Ibrahim, S. Khalid, K. Idrees, Arab J Chem 12(7), 908 (2019)

[5] Z. Khodaparast, S. Pashaei, S. Mohammadi-Aghdam, H. Reza Azimi, S. Hosseinzadeh, J Inorg Organomet Polym Mater 30, (2020); https://doi.org/10.1007/s10904-019-01243-8

[6] A. Sankaran A, K. Kumaraguru K, B. Balraj B, J Inorg Organomet Polym Mater 31, 151 (2021); https://doi.org/10.1007/s10904-020-01655-x

[7] R.D. Pyarasani, T. Jayaramudu, A.J. Jhon, Mater Sci, 54, 974 (2019) https://doi.org/10.1007/s10853-018-2977-x

[8] U. Bogdanovic, V. Vodnik, M. Mitric, ACS Appl Mater Interfaces 7, 1955 (2015) https://doi.org/10.1021/am507746m

[9] K. Pandiselvi, S. Thambidurai, Colloids Surf B 108, 229 (2013)

[10] S.M. Ebrahimzadeh Sepasgozar, S. Mohseni, B. Feizyzadeh, A. Morsali, Bull Mater Sci 44,

129 (2021); https://doi.org/10.1007/s12034-021-02419-0
[11] G. Zhang, H. Zheng, M. Shen, L. Wang, X.J. Wang, Phy Chem Solids 81, 79 (2015); https://doi.org/10.1016/j.jpcs.2014.12.012
[12] A. Romero-Montero, M. Gimeno, N. Farfan, P.J. Labra-Vazquez, Mol Struct 1197, 326 (2019); https://doi.org/10.1016/j.molstruc.2019.07.050
[13] C. Ceylan Kocak, S. Ulubay Karabiberoglu, Z. Dursun, J Electroanal Chem 853, 11355 (2019)
[14] E. Parthiban, N. Kalaivasan, S. Sudarsan, Arab J Chem 13, 4751 (2020); https://doi.org/10.1016/j.arabjc.2019.12.002
[15] R. Jayasree, A. Vasantharaja, B. Abirami, Wound Med 27, 100170 (2019); https://doi.org/10.1016/j.wndm.2019.100170
[16] S. Shaik, M. Rao Kummara, S. Poluru S, C. Allu, J. Mohiddin Gooty, C. Rao Kashayi, M. Chinna Subbarao Subha, Int J Carbohydr Chem 11, 1 (2013); https://doi.org/10.1155/2013/539636
[17] S. Tajik, H. Beitollahi, M. Reza Aflatoonian, B. Mohtat, B. Aflatoonian, I. Sheikh Shoaie, M.A. Khalilzadeh, M. Ziasisistani, K. Zhang, H. Won Jang, M. Shokouhimehr, RSC Adv 10, 15171 (2020); https://doi.org/10.1039/D0RA02380A
[18] G. Hitkari, P. Chwdhary, V. Kumar, S. Singh, A. Motghare, Clean Chem Eng 1, 100003 (2022); https://doi.org/10.1016/j.clce.2022.100003
[19] J. Varghese, K.T. Varghese, Mater Chem Phys 167, 258 (2015); https://doi.org/10.1016/j.matchemphys.2015.10.041
[20] B. Rathore, N. Pal Singh Chauhan, M. Rawal, S. Ameta, R. Ameta, Polym Bull 77, 2 (2020); https://doi.org/10.1007/s00289-019-02994-7
[21] A. Olad, S. Behboudi, A. Entezami, Bull Mater Sci 35, 801 (2012); https://doi.org/10.1007/s12034-012-0358-7
[22] W.C. Oh, K. Nahar Fatema, Y. Liu, C. Sung Lim, K. Youn Cho, C.H. Jung, M.J. Rokon Ud Dowla Biswas, Photochem Photobiol A: Chem 394, 112484 (2020); https://doi.org/10.1016/j.jphotochem.2020.112484
[23] K. Basavaiah, M.D. Prasad, A.V. Prasada Rao, J Exp Nanosci 9, 491 (2014); https://doi.org/10.1080/17458080.2012.670276
[24] A. Janosevic Lezaic, I. Pasti, A. Gledovic, J. Antic-Stankovic, D. Bozic, S. Uskokovic-Markovic, G. Ciric-Marjanovic, Syn Met 286, 117048 (2022)
[25] K. Tamilselvi, K. Alamelu Mangai, M. Priya, S. Sagadevan, Chem Phys Lett 765, 138320 (2021); https://doi.org/10.1016/j.cplett.2021.138320
[26] S. Raja, M. Deepa, Indian J Adv Chem Sci 3, 198 (2015)
[27] V.S. De Souza, H.O. Da Frota, E.A. Sanches, J Mol Struct 1153, 20 (2018); https://doi.org/10.1016/j.molstruc.2017.09.084
[28] A.M. Shano, I.M. Ali, N.A. Bakr, J Nano-Electron Phys 11, 06016 (2019)
[29] M. Fuseini, M.M. Yousry Zaghloul, M.F. Elkady, A.H. El-shazy, J Mater Sci 57, 6085 (2022); https://doi.org/10.1007/s10853-022-06994-3
[30] D.M. Jundale, S.T. Navale, G.D. Khuspe, D.S. Dalavi, P.S. Patil, V.B. Patil, J Mater Sci: Mater Electron 24, 3526 (2013); https://doi.org/10.1007/s10854-013-1280-5
[31] E. Parthiban, N. Kalaivasan, S. Sudarsan, J Inorg Organomet Polym Mater 30, 4677 (2020); https://doi.org/10.1007/s10904-020-01602-w
[32] V. Vinod Kumar, A. Dharani, M. Mariappan, S. Philip Anthony, RSC Adv 6, 85083 (2016); https://doi.org/10.1039/C6RA16553B
[33] S.P. Ashokkumar, L. Yesappa, H. Vijeth, M. Niranjana, M. Vandana, H. Devendrappa, Mater Res Express 6, 125557, (2019); https://doi.org/10.1088/2053-1591/ab5dde
[34] Z. Neisi, Z. Ansari-Asl, A.S Dezfuli,s J Inorg Organomet Polym Mater 29,1838-1847 (2019); https://doi.org/10.1007/s10904-019-01145-9
[35] P. Linganathan , J. Sundararajan, J. Mary Samuel,s J Compos Sci 1-9 (2019)

[36] S. Das, V. Chandra Srivastava, Mater Sci Semicond Process 57:173-177 (2017); https://doi.org/10.1016/j.mssp.2016.10.031

[37] Y. Wang, D. Fan, D. Wu, Y. Zhang, H. Ma, B. Du, Q. Wei Sen and B. Actuators : Chem 236:241-248 (2016); https://doi.org/10.1016/j.snb.2016.06.021

[38] M. Bhushan, Y. Kumar, L. Periyasamy, A.K. Viswaanath Mater Sci Eng: C 96:66-76 (2019); https://doi.org/10.1016/j.msec.2018.11.009

[39] M.J. Hajipour, K.M. Fromm, A.A Ashkarran, D. Jimenez de Aberasturi, I.R.D. Larramendi, T. Rojo, V. Serpooshan, W.J. Parak, M. Mahmoudi Trends Biotechnol 30:499-511 (2012); https://doi.org/10.1016/j.tibtech.2012.06.004

[40] H. Qamar, S. Rehman, D. Chauhan, A. Tiwari, V. Upmanyu Int J Nanomedicine 15:2541-2553 (2020); https://doi.org/10.2147/IJN.S240232

[41] M.L. Knetsch, L.H. Koole Polymers 3:340-366 (2011); https://doi.org/10.3390/polym3010340

[42] K.M. Manesh, A.I. Gopalan, K.P. Lee, S. Komathi Catal Commun 11:913-918 (2010); https://doi.org/10.1016/j.catcom.2010.03.013

[43] Y. Chi, Q. Yuan, Y. Li, J. Tu, L. Zhao, N. Li, X. Li, J. Colloid Interface Sci 383: 96-102 (2012); https://doi.org/10.1016/j.jcis.2012.06.027

[44] M. Ayad, W.A. Amer, M.G. Kotp Mol Catal 439:72-80 (2017); https://doi.org/10.1016/j.mcat.2017.06.023

[45] X. Zhang, W.X. Zhi, B. Yan, X. Xu Powder Technol 221:177-182 (2012); https://doi.org/10.1016/j.powtec.2011.12.064